ELSEVIER

Thin Solid Films 322 (1998) 167–176

thin solid films

Effect of coupling of radio-frequency plasma on the growth of diamond films in a hot filament reactor

M.P. Pai [a], D.V. Musale [a], S.T. Kshirsagar [a,*], A. Mitra [b], S.R. Sainkar [b]

[a] *Physical and Materials Chemistry Division, National Chemical Laboratory, Pune 411 008, India*
[b] *Special Instruments Lab., National Chemical Laboratory, Pune 411 008, India*

Received 26 August 1997; accepted 30 October 1997

Abstract

Diamond films have been deposited using a chemical vapour deposition (CVD) technique involving a hybridization of the hot filament and the capacitively coupled radio-frequency (RF) plasma. The changes produced in the surface morphology and Raman spectra of these films are investigated as a function of the magnitude of RF power and deposition chamber pressure. The coupling of low levels of RF power with the hot filament CVD is observed to improve the growth rate as well as quality of the diamond films while higher levels of RF power decreased the growth rate and produced porous films containing needle-shaped microcrystals. These changes are attributed to the ion bombardment of the growing film due to the self-biasing effect of the RF plasma.

Keywords: Chemical vapour deposition (CVD); Diamond; Glow discharge; Raman scattering

1. Introduction

The natural and synthetic (grown in high pressure–high temperature reactor) diamond, by virtue of its wide band gap ($\sim$ 5.4 eV), is predicted to have higher carrier mobility ($\sim$ 2000 $cm^2\ V^{-1}\ S^{-1}$), high breakdown voltages, saturated drift velocities, strong radiation and mechanical hardness, and highest thermal conductivity (20 $W\ cm^{-1}\ K^{-1}$) and thus offers almost ideally suited solid state material choice for semiconductor device applications which involve extreme temperature and environmental conditions [1,2]. Because of these unusual properties and its commercial importance, synthetic diamond production has long been a goal of numerous organizations. A considerable success has recently been achieved in the production of polycrystalline diamond films by employing the simple low-pressure low-temperature chemical vapour deposition (CVD) techniques. There are, in fact, many versions of the CVD reactors that can be used for the stable growth of well-crystallized diamond films, but at the moment the microwave plasma assisted CVD (MW-CVD) [3a,3b,4] and the hot-filament assisted CVD (HF-CVD) have shown considerable promise for the commercial production. There are, however, practical limitations to the use of microwaves: viz. the difficulty in 'scaling up' the plasma to enable the growth of large area films (> 10 cm diam.). The HF-CVD is capable of producing large area films ($\sim$ 30 cm diam.) [5] but it renders growth rates lower than those of MW-CVD. On the other hand, when the diamond growth was attempted by using the capacitively coupled radio-frequency (RF) plasma assisted CVD (RF-CVD) technique, the deposited material had extremely poor quality [6a,6b,6c]. Although, Wood et al. [7] have reported some work on the diamond growth by RF-CVD, major potential of this industrially acceptable technique has remained untapped. The ion-bombardment caused due to the self-biasing effects in the RF-plasma appears to be the probable detrimental parameter for the poor quality diamond growth. The bombarding ions can induce lattice disorder which eventually can transform the higher energy metastable sp^3 bonded carbon with diamond phase into the lower energy stable sp^2 bonded carbon in graphitic phase and thus may hinder the nucleation. In contrast, recent studies on the use of positive or negative dc bias, which ensures some kind of particle bombardment in MW-CVD or HF-CVD, have revealed the enhancement of the nucleation densities and growth rates [8,9,10a,10b,11]. It is, therefore, felt necessary to perform more experimental

* Corresponding author.

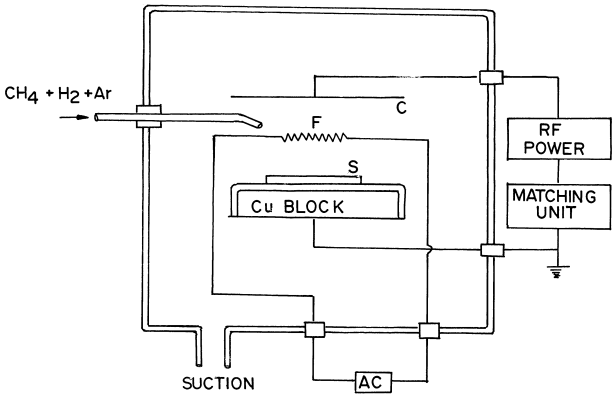

Fig. 1. The schematic diagram of the RF–HF-CVD reactor; C—Cathode, F—tungsten filament, S—Substrate, AC—Power for Filament, Cu block —Heat Sink.

investigations on the deposition of diamond films by RF plasma techniques. We have attempted the production of diamond films using a 'hybrid RF plasma plus hot-filament' reactor [12–14] and report here the results of the studies on the effect of coupling of RF-plasma on the growth of diamond films in such a modified hot-filament CVD reactor.

2. Experimental

The HF-CVD system used in the present study consists of a high vacuum stainless steel (SS) chamber at the centre of which a M-shaped planar filament made out of tungsten wire (500 μm SWG) was positioned [14] (see Fig. 1). The substrate holder made out of a mild steel (MS) plate was placed in contact with a copper block (heat sink) which enabled to maintain substrate temperature at $\sim 900^{\circ}$C. The RF electrodes made out of Mo/Ni sheets were placed about the filament in a parallel plate capacitor-like configuration. One of these electrodes forms the substrate holder. The spacing between these electrodes can be adjusted so that for a given gas pressure a bright RF glow could be excited between the plates. The distance between the fila-

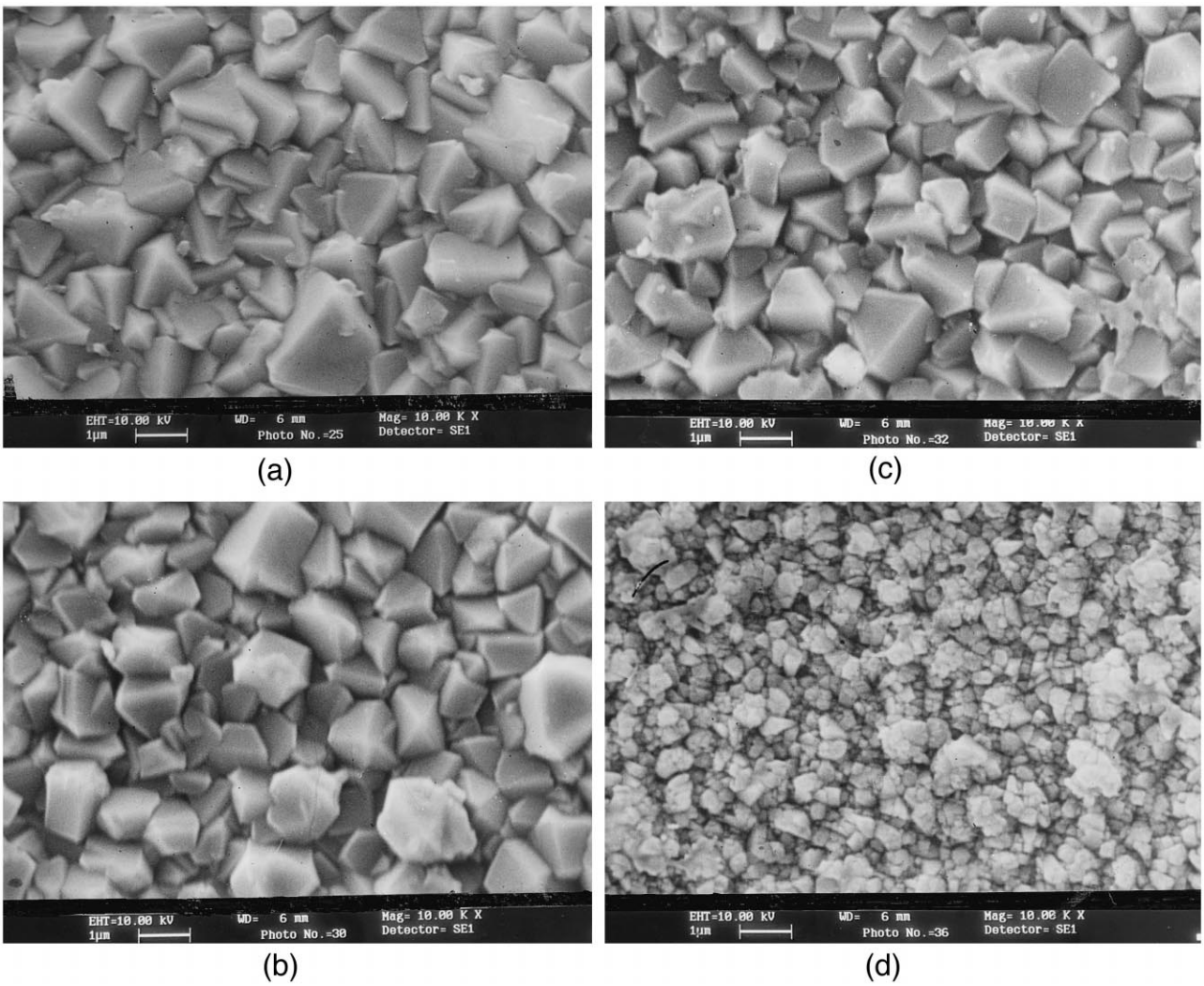

Fig. 2. SEM photograph of the diamond films deposited at chamber pressure of 40 Torr and RF power (a) 0 W, (b) 10 W, (c) 20 W, and (d) 40 W.

ment and the substrate surface was kept constant at 10 mm. The gas mixture was introduced through a SS tube (5 mm ID) that opens just near the filament. The filament was energized with 50 Hz power through an isolation transformer while the RF electrodes were supplied with the 13.56 MHz power through a L-C matching network. The polarity of the substrate holder could be changed from that of the ground electrode to a RF electrode depending upon the experimental requirements.

The gas flow and pressure were measured by using the electronic mass flowmeters and Baratron pressure gauge respectively. The source gas mixture was $\sim$2% Methane by volume in H_2 or in H_2 + Argon.

The substrate temperature (T_s) was measured by a standard Pt/Pt–Rd 13% thermocouple while the filament temperature (T_F) was measured by using an optical pyrometer. The application of RF plasma was observed to increase the T_S and T_F slightly and therefore the electrical power parameters were adjusted after the excitation of the plasma so that the deposition conditions could be maintained uniform for a comparative study of the films deposited with or without the RF plasma.

The optically polished C–Si ⟨111⟩ substrates were subjected to a light abrasion with 1 μm size diamond powder and subsequently degreased in acetone and rinsed in 40% HF acid solution prior to their loading in the deposition chamber.

The Raman scattering (Ramalog Spectrometer SPEX-1403 with Third Monochromator), using the argon-ion-laser (Spectra Physics 168 B) radiation (514.5 nm) as an excitation source, was used to characterize the film composition in terms of the proportions of sp^3 bonded (diamond-like) carbon relative to that of the sp^2 bonded (graphitic) carbon. The details of the Raman apparatus and measurements are described elsewhere [15,16]. The (Leica stereo scan 440) Scanning Electron Microscope was used to photograph the surface morphological changes as a function of various deposition conditions. Film thickness was

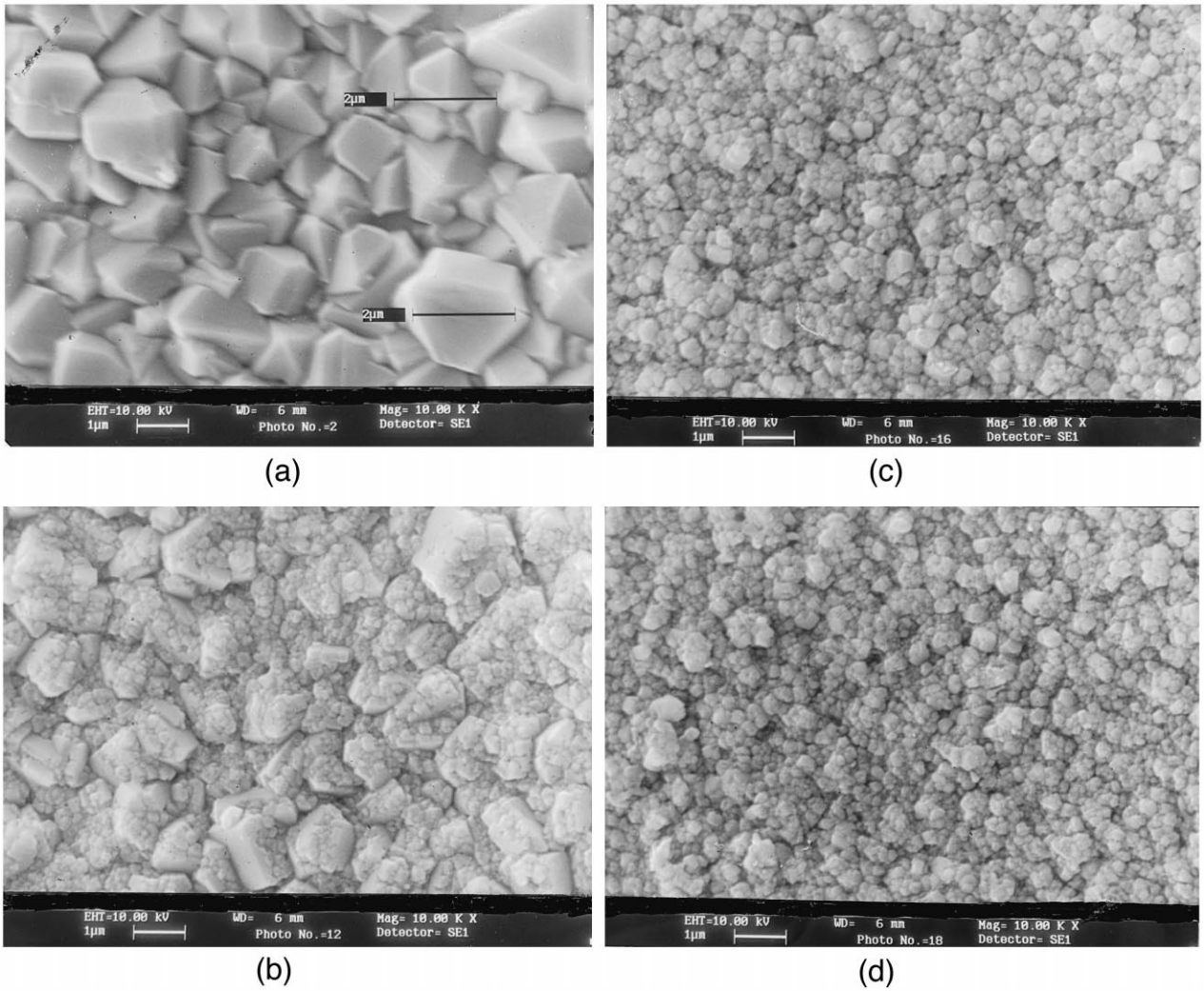

Fig. 3. SEM photograph of the diamond films deposited at chamber pressure of 30 Torr and RF power (a) 0 W, (b) 10 W, (c) 20 W, and (d) 40 W.

measured by the weight method and confirmed by the SEM measurements of its cut cross section.

3. Results and discussion

3.1. Morphology: scanning electron microscopy

The unique characteristic of diamond films synthesized by the CVD technique is that the crystal habits and surface morphology strongly depend on the experimental conditions. We have, therefore, taken necessary care to maintain the common deposition parameters as uniform as possible for all the deposition experiments e.g. (a) 294 SCCM of H_2 flow (b) 6 SCCM of CH_4 flow (c) $T_F = 1970 \pm 20°C$ (d) $T_s = 780 \pm 10°C$ and (e) the deposition time period of 180 min. Moreover, the spread of the RF plasma with reference to the RF electrode depends on the chamber pressure as well as on the magnitude of RF power and hence the film deposition in the RF–HF-CVD system was mainly carried out by keeping the chamber pressure constant at one of the following values, 40 Torr, 30 Torr, or 20 Torr while the RF power was varied as 0 W (i.e. only the HF-CVD), 10 W, 20 W and 40 W. These experimental conditions have generated three sets of diamond films and as such enabled us to reliably correlate the changes occurring in the morphology to the RF power alone. The surface of the films synthesized for 3 h at different RF powers but at a constant chamber pressure were then observed by the SEM.

Figs. 2a, 3a and 4a reveal the surface of the diamond films grown only by the HF-CVD for respective gas pressure of 40 Torr, 30 Torr and 20 Torr. The surface morphology of these HF-CVD films appears to have common features which indicate that the surface is made up of closely packed large triangular pyramidal shaped diamond particles with well developed {111} facets. Most of these particles are not single crystals but have twin structure [17]. Another observation is that the surface morphology is relatively insensitive to the chamber pressure used for the

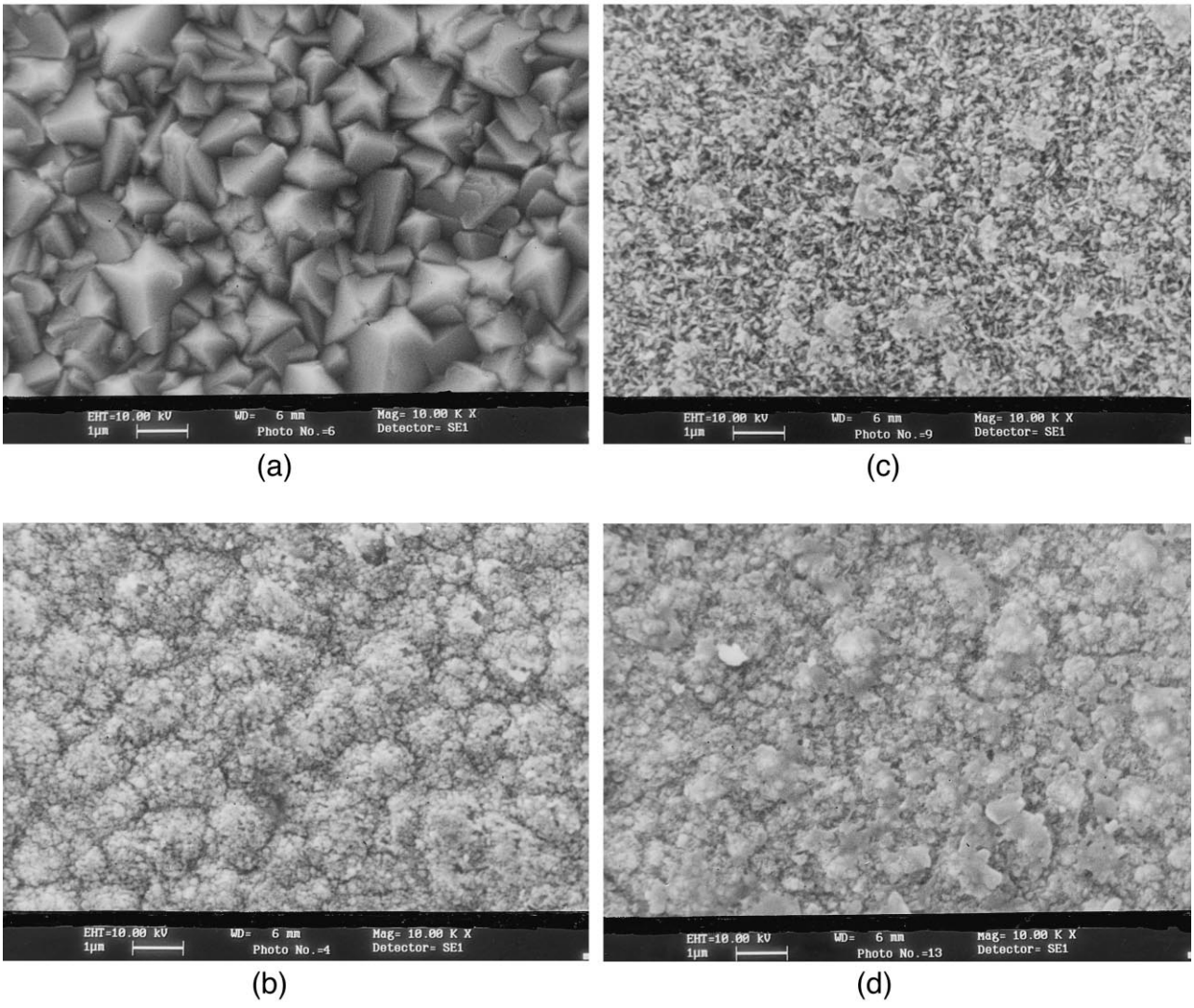

Fig. 4. SEM photograph of the diamond films deposited at chamber pressure of 20 Torr and RF power (a) 0 W, (b) 10 W, (c) 20 W, and (d) 40 W.

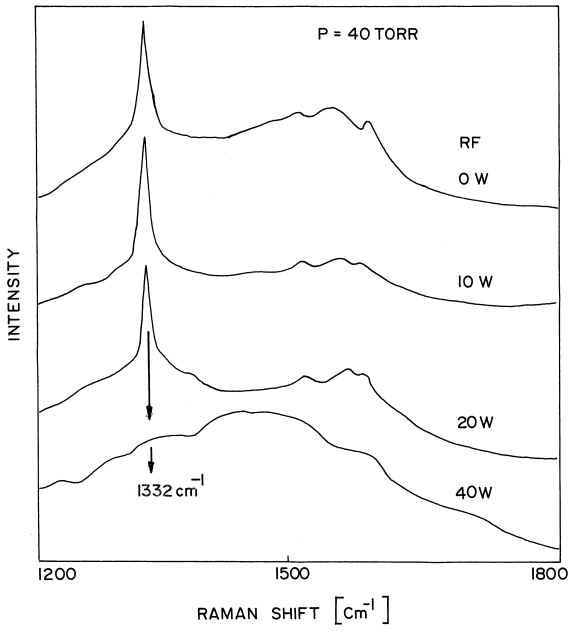

Fig. 5. Raman spectra of the diamond films deposited at chamber pressure of 40 Torr and RF power of 0 W, 10 W, 20 W, and 40 W.

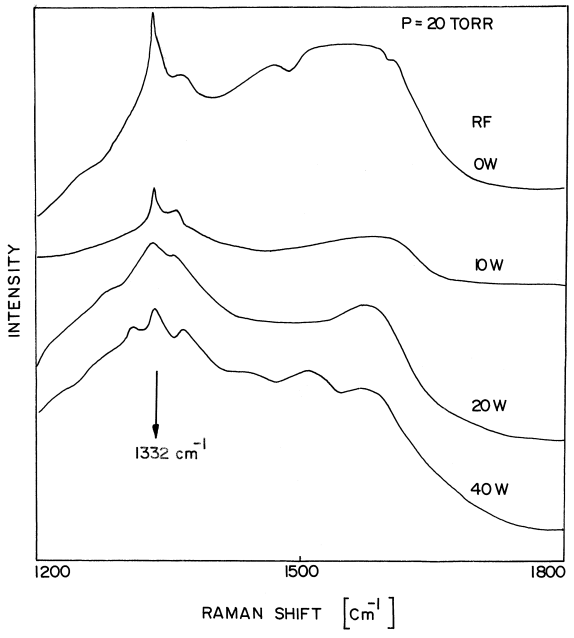

Fig. 7. Raman spectra of the diamond films deposited at chamber pressure of 20 Torr and RF power of 0 W, 10 W, 20 W, and 40 W.

HF-CVD. These results confirm the morphological reproducibility of our HF-CVD films and suggest that it is possible for us to reliably correlate to the magnitude of RF power the changes produced in the surface morphology on imposition of the RF plasma.

The SEM pictures shown in Figs. 2–4 show that the surface morphology is, in general, seen to undergo a drastic change when the film is grown under the RF-plasma hybridization condition. The large grained polycrystalline morphology with mixed cubo–octahedral and triangular pyramidal crystals having well developed {111} facets as observed in the HF-CVD films is seen to change at low RF powers into a morphology consisting of the mixed fine cubo–octahedral shaped single or twin crystals but with the triangular pyramid type crystals disappeared. For higher RF power the submicron cauliflower-like microcrystalline clusters are seen to appear. The surface morphology is further affected by the chamber pressure which influences the spread of the RF plasma. The effect of the RF-plasma on the surface morphology appears to be weaker when the gas pressure is greater than 30 Torr, while it is pronounced when the pressure is less than 20 Torr. The details of the changes in morphology as a function of the RF power are described in the following

In Fig. 2, we show the surface morphology as revealed by the SEM for the films grown by keeping the gas pressure constant at 40 Torr and varying the RF power

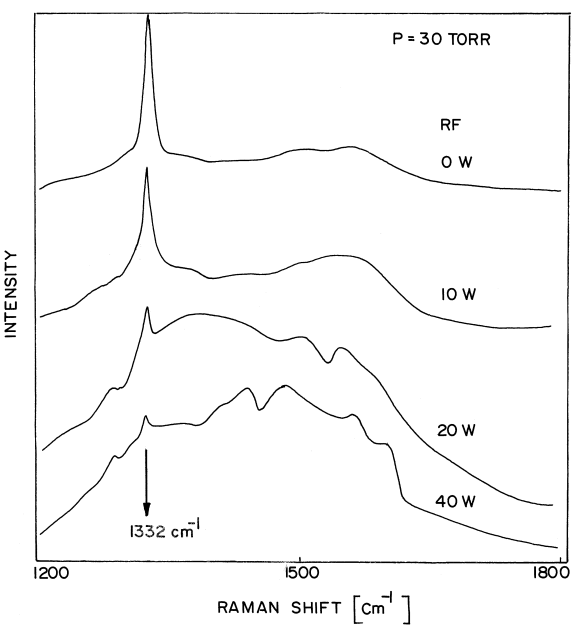

Fig. 6. Raman spectra of the diamond films deposited at chamber pressure of 30 Torr and RF power of 0 W, 10 W, 20 W, and 40 W.

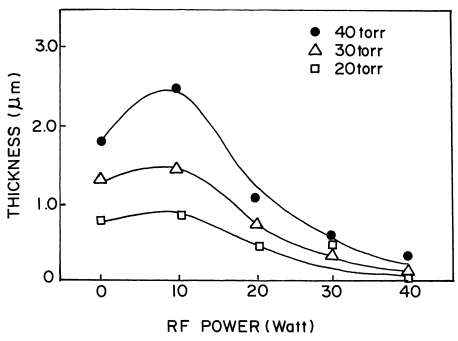

Fig. 8. Growth rate as a function of RF power.

from 0 to 40 W. The 0 W (HF-CVD)films are seen to have the surface morphology consisting of the densely packed mixed twins of the cubo–octahedral and the triangular pyramid type crystallites with their vertices pointing outward. The imposition of the RF plasma is seen to affect the spatial packing density of the crystallites. For the RF power of 10 W and 20 W, there is reduction in the twinning effect as well as in packing density of the crystallites. Moreover, the crystallites are seen to grow bigger in size with increased separation between them. There is also a change in the crystallite orientation with respect to the substrate surface, e.g., the pyramidal shaped crystals start disappearing and their place is taken by the crystals with faces ({111} and {100}) lying parallel to the substrate surface. This change in the morphology may be attributed to the increase in the concentration of carbon species in the deposition region caused due to the additional dissociation of CH_4 by the RF plasma [18–20]. Alternately, the voids or the separations (dark portions) in the film surface are seen to increase with the increase of RF power. On the other hand, films grown with RF power ≥ 30 W have shown presence of submicron crystallites with cubo–octahedral twins and multiple secondary nucleation. It is, however, interesting to note that the original underlying geometrical distribution (layout) of the crystals or grains appears to remain more or less same. This underlying structure may be attributed to the contribution from the HF-CVD deposition process. The featureless grains may be expected to contain microcrystalline and/or amorphous material as revealed by the Raman spectra shown in Fig. 5, the details of which are discussed in Section 3.2.

The SEM pictures of the surface morphology of the films grown at chamber pressure of 30 Torr with different magnitudes of RF powers, are shown in Fig. 3a–d. The

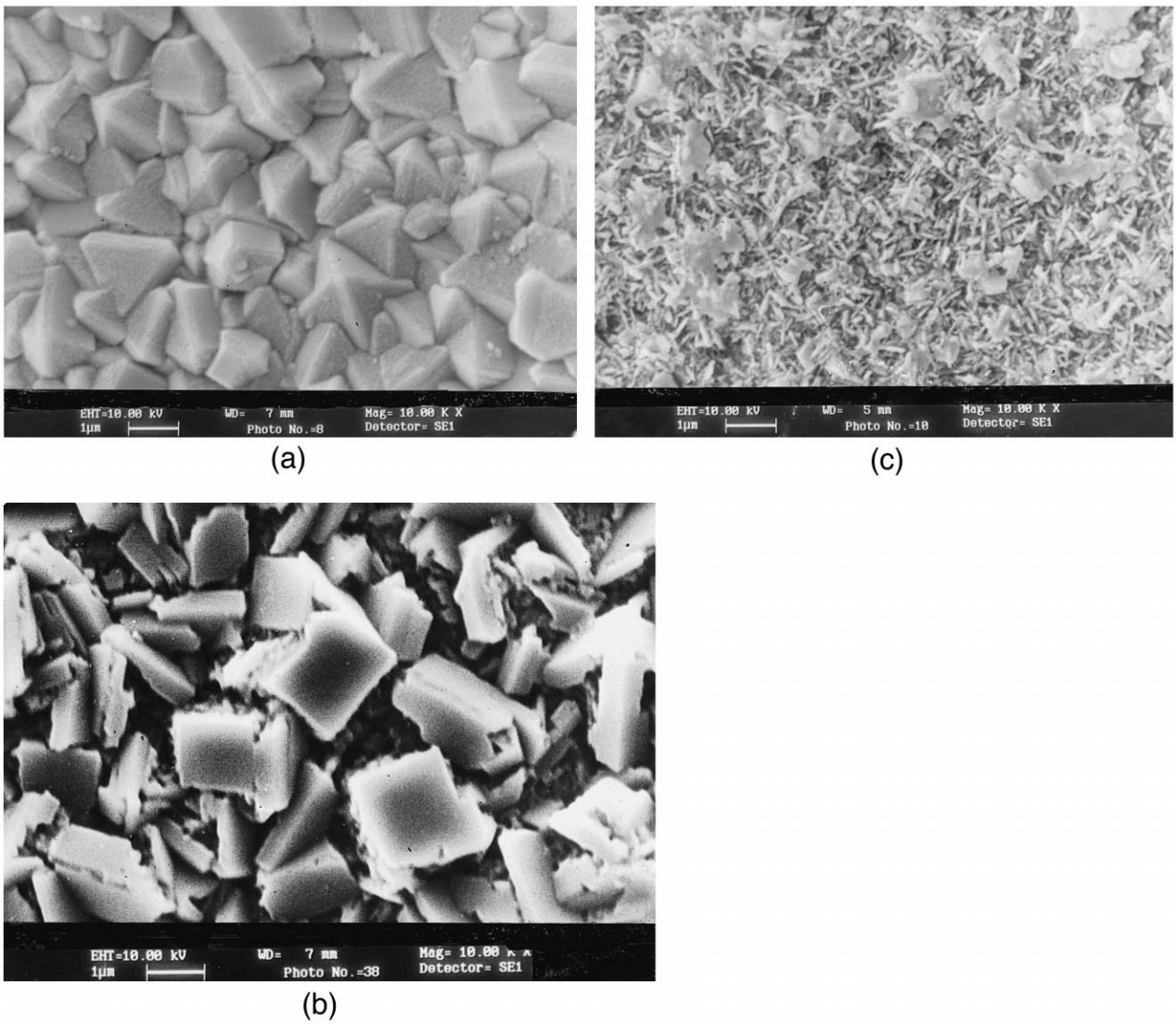

Fig. 9. SEM photograph of surface morphology of the diamond films deposited at 30 Torr pressure in HF-CVD (a) with 200 SCCM of H_2 + 100 SCCM of Ar + 6 SCCM of CH_4; and in RF–HF-CVD at 30 W of RF power with (b) 240 SCCM of H_2 + 60 SCCM of Ar + 6 SCCM of CH_4 and (c) 200 SCCM of H_2 + 100 SCCM of Ar + 6 SCCM of CH_4.

HF-CVD films grown for pressure of 30 Torr appear to have the surface consisting of closely packed clean cubo–octahedral crystallites. The RF–HF-CVD films deposited at RF power of 10 W, 20 W, and 40 W display the mixed morphology due to the big diamond crystallites and the submicron secondary multi-nucleation. At 10 W of RF power, the surface appears as if the big diamond crystallites got covered with a low density submicron particulates while at 20 W and 40 W of RF power, the submicron particulate phase is seen to dominate the surface morphology. The geometrical grain distribution (layout) as observed in the HF-CVD films still appears to be maintained for this set of samples also. The Raman spectra of these films are shown in Fig. 6.

As the chamber pressure is reduced further to 20 Torr, the films grown under the RF plasma display the surface morphology consisting of featureless particles or clusters with cauliflower-like structure having reduction in the packing density of the crystallites (see Fig. 4). The surface becomes more porous with the increase of RF power. The original underlying geometry of the grain distribution as seen in the HF-CVD films is no longer present in these RF–HF-CVD films. However, needlelike microcrystals are now seen clearly in the films grown at the RF power of 20 W and 40 W. The Raman spectra of these films are compared in Fig. 7.

3.2. Raman measurements

The Raman Spectra of the films deposited by RF–HF-CVD are compared with the corresponding HF-CVD films in Figs. 5–7. These spectra, in common, exhibit sharp bands at $\sim$1330 cm^{-1} and broad bands in the ranges 1250 cm^{-1}–1400 cm^{-1}, and 1450–1600 cm^{-1}. These spectra are clearly different from the characteristic spectra of the individual crystalline carbon phases such as the diamond and graphite. The diamond displays a single sharp Raman line at 1332 cm^{-1} [21], whereas the large graphite crystals show a single sharp Raman line at 1580 cm^{-1} known as ‘G’ line [22]. When the graphite crystal is small, it gives additional sharp line, called ‘D’ line, at 1355 cm^{-1} having extremely low strength compared to the ‘G’ line [23,24]. Moreover, the frequency, width and relative strength of the ‘D’ and ‘G’ bands are known to vary with the crystallite size [25].

The Raman spectra of most of our samples may be considered to be formed by the superimposition of characteristic features of both the diamond-like and graphite-like phases with the difference that these features appear here comparatively more broad. We, therefore, believe that these spectra have additional scattering coming from the diamond-like amorphous carbon [26] which generally display a broad band centered at about 1530 cm^{-1} (G-like band) with a broader shoulder centered at 1380 cm^{-1} (D-like band) [27]. In addition to these amorphous features, we observe much more broader G-like and D-like bands so that the dip between them appears to be filled up when either the RF-power is increased or the pressure decreased. These results show qualitative similarity to the Raman spectra of the ion bombarded diamond and graphite crystals reported by Lee et al. [28]. The G-like and D-like bands are seen to coalesce into a broad asymmetric band with the D-like band blue shifted and the G-like band red shifted. This is an opposite behaviour compared to that seen in the changes in the Raman spectra when the graphite particle size was made to diminish [23,24]. The low intensities of ‘D’ band relative to the ‘G’ band intensities represent an improvement of order [29]. The Raman spectra of our films may thus be conjectured to be formed by the superimposition of various broad bands discussed above. Nevertheless, the special feature that all of these spectra share in common is the presence of strong D-like broad band peaking at $\sim$1330 cm^{-1} with the G-like band more broadened in width and weakened in strength.

The Raman spectra of the HF-CVD films (Curve I in Figs. 5–7) show a sharp but strong band at 1332 cm^{-1} overlapping the ‘D’-like broad band at 1350 cm^{-1} and a broad but weak band at about 1540 cm^{-1}. The 1332 cm^{-1} band indicates presence of the diamond crystals while the broad G-like band, which in fact is composed of number of broad bands, indicates presence of the amorphous carbon. However, the relative strengths of these bands cannot be taken as the direct measure of their concentrations in the film as their scattering cross sections as well as absorption coefficients are different [30,31]. Thus, when the Raman band at 1332 cm^{-1} is enhanced by an appropriate factor

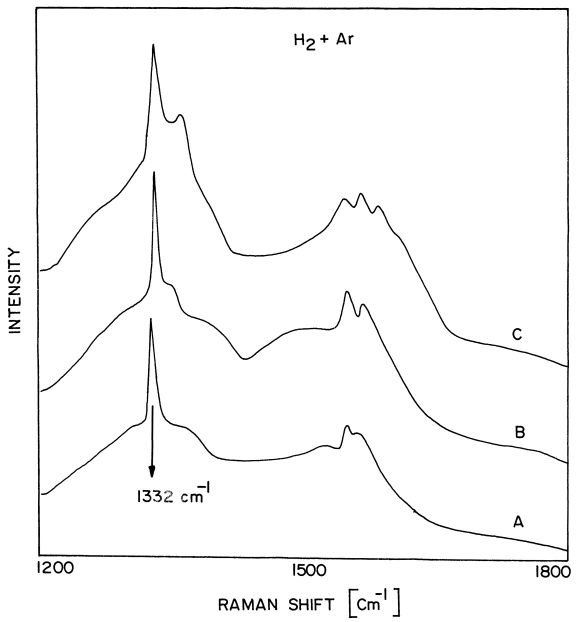

Fig. 10. Raman spectra of the diamond films deposited by adding argon to source gas: at Pressure of 30 Torr in HF-CVD with (A) 200 SCCM of H_2 + 100 SCCM of Ar, and in RF–HF-CVD at 30 W of RF power with (B) 240 SCCM of H_2 + 60 SCCM of Ar and (C) 200 SCCM of H_2 + 100 SCCM of Ar.

would show that the amorphous and crystalline graphite bands shall have extremely low strengths and thus their concentration be negligible. This could also be the reason why the SEM pictures of these HF-CVD film appear clean and free from amorphous coating on the crystallites.

In Fig. 5 we compare the Raman spectra of the RF–HF-CVD films grown at the chamber pressure of 40 Torr and different RF powers. The 10 W film shows a strong band at 1332 cm^{-1} while the G-like band appears to be suppressed compared to that of HF-CVD film. Hence, the RF-plasma at low power level appears to enhance the quality of the film which is also clearly seen in the SEM pictures in Fig. 2. As the RF power is increased further, the contribution of D-like and G-like bands also increases. For the RF power beyond 30 W these bands become so strong that the 1332 cm^{-1} band becomes apparently invisible and thus suggests the absence of diamond crystals. However, the SEM pictures show some presence of diamond crystals though they may be coated or embedded in the amorphous carbon clusters. These results lead to a conjecture that the imposition of RF-plasma at 40 Torr, may improve the quality of the film at low RF powers but may degrade it for higher levels. The Raman spectra of RF–HF-CVD films deposited at lower pressures, viz. 30 Torr and 20 Torr, also show similar behaviour (see Figs. 6 and 7). The Common features of all these spectra are: i) the region of D band has higher strength than that of the G-region and ii) the D-band appears to peak at 1332 cm^{-1} while the G-band peak becomes broad. These features thus indicate that the microcrystals of diamond can be present in all these films along with certain amount of amorphous carbon.

The weaker G-like band and the stronger D-like band with the dip between them filled up by additional bands are the additional features of these spectra. It is difficult to deconvolute such complex spectra [32,33]. Hence at present it may be possible to visualize that these films are likely to have much higher component of sp^3 bonded

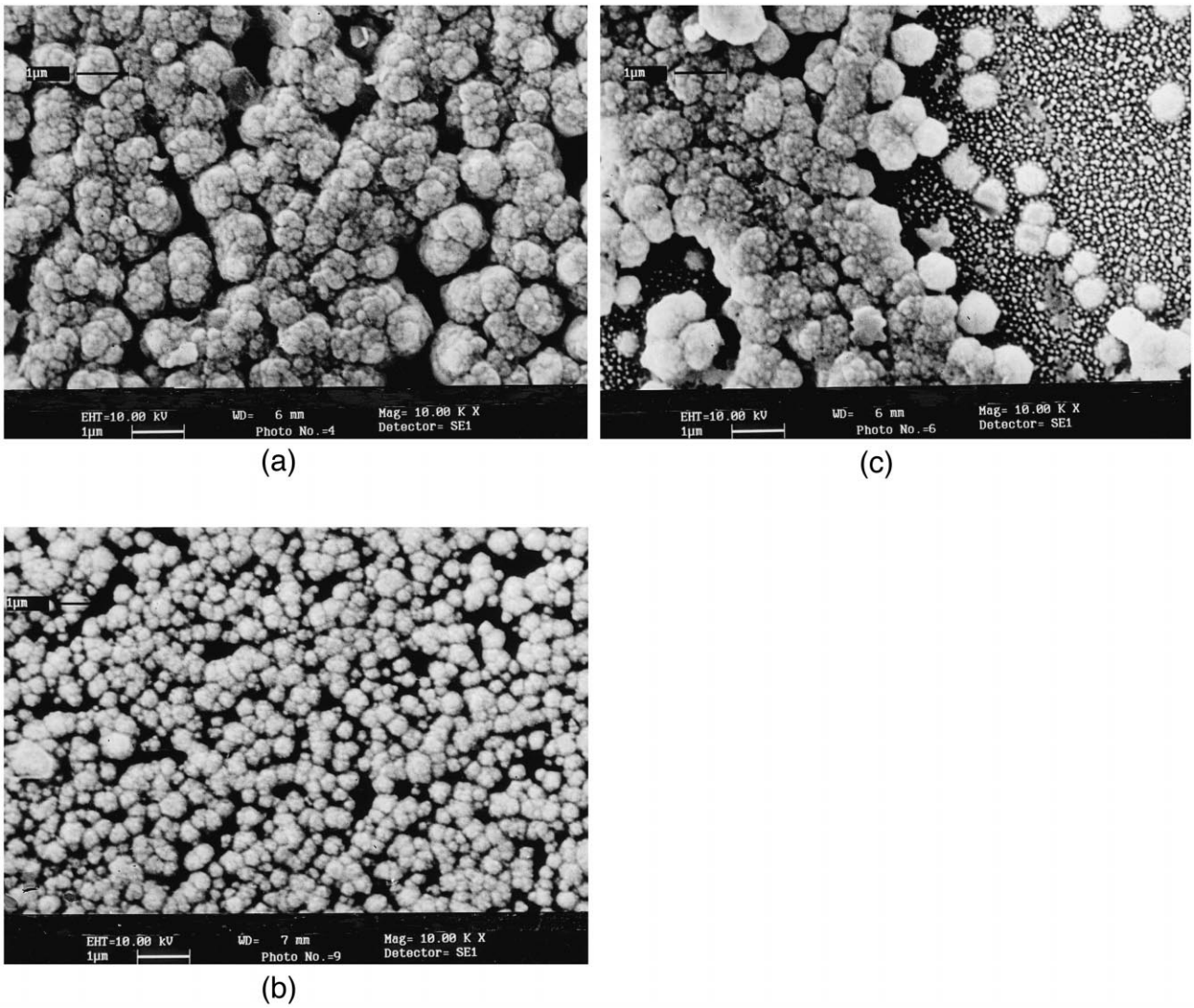

Fig. 11. SEM photograph of surface morphology of the diamond films deposited with RF-potential applied to substrate holder: Rf power: (a) 10 W, (b) 20 W and (c) 30 W.

carbon compared to the films previously produced by the RF-CVD or the sputter deposition techniques [32]. Hence the composition of the films produced by RF–HF-CVD may be believed to have the microcrystalline diamond dispensed in a weak amorphous matrix of carbon clusters.

The imposition of RF-plasma may be acting in three ways: (a) The plasma can dissociate the H_2 molecules and thus acts as an additional source of atomic Hydrogen whereas in the HF-CVD the hot filament is the only source of atomic hydrogen (b) The plasma increases the decomposition of CH_4 leading to the increase of carbon-species in the region between filament and substrate, and thus enhances deposition rate of the carbon species (see Fig. 8) and (c) The plasma gives rise to the ion-bombardment of the film leading to the physical sputtering of the deposited film as well as H induced chemical etching of the growing film, thus reducing the diamond growth rate for higher levels of RF power. The increased atomic hydrogen can lead to better growth of diamond crystallites at low RF-powers. At higher RF powers and lower pressure, the mean free path of the ions bombarding the films increases and thus can cause removal of loosely bonded carbon which may be present in the amorphous sp^2 bonded phase. This process may be considered to lead to the formation of voids and gaps in the film as shown by the SEM pictures in Figs. 2 and 3. The films prepared by RF–HF-CVD at 20 Torr or less are seen to be completely porous with absence of well defined crystallites. The Raman spectra, however, indicate presence of diamond particles due to the peaking of D-band at 1332 cm^{-1} and drastic reduction in strength of G-bands. We, therefore, conclude that the hybrid technique allows growth of diamond films containing submicron size microcrystalline particles which may not be possible to characterize by the X-ray diffraction techniques.

In order to supplement our above conjectures with more experimental evidence, we have prepared films by introducing Ar in the deposition chamber along with $H_2 + CH_4$ source gas. We expected the Ar to ionize easily in the RF plasma and provide additional intense ion-bombardment. Fig. 9a shows the SEM picture of HF-CVD film deposited by using (a) 200 SCCM of H_2, 100 SCCM of Ar and 6 SCCM of CH_4. These films show usual surface morphology consisting of closely packed mixture of cubo–octahedral and triangular pyramidal crystallites similar to those of the HF-CVD films deposited from the $H_2 + CH_4$ gas mixture. The SEM pictures of the RF–HF-CVD films grown by using (b) 240 SCCM of H_2, 60 SCCM of Ar and 6 SCCM of CH_4, and (c) 200 SCCM of H_2, 100 SCCM of Ar and 6 SCCM of CH_4 are shown in Fig. 9b and c, respectively. For both of these depositions, the RF power and chamber pressure were maintained at 30 W and 30 Torr respectively while the rest of the deposition parameters were the same as mentioned earlier. Fig. 9b reveals that the moderate Ar concentration has changed the surface morphology from that of the mixture of closely packed of cubo–octahedral and triangular pyramidal crystallites with large facets of {111} orientation (as observed in the HF-CVD films) to that of a cubic type crystallites with large {100} facets. Such transitions have been observed when concentration of carbon species was increased in the deposition zone [19]. The voids are also seen to increase drastically with Argon concentration in the gas mixture. Further increase of Ar concentration is seen to produce films having highly porous structure and the morphology consisting of needle shaped crystallites as has been observed for the films grown at low pressures and high RF power levels. The Raman spectra (see Fig. 10) again show the features similar to those of other RF–HF-CVD films characterized by the broad 'D'-like band peaking at 1332 cm^{-1} and broad G-like band having very low strength. These results imply that the moderate ion-bombardment in RF–HF-CVD films helps in removing weakly (sp^2) bonded carbon.

Further evidence for ion bombardment is obtained from the deposition experiments in which the RF power was supplied to the electrode that supported the substrates. A cauliflower-like growth was observed (see Fig. 11). On increase of RF power the films appeared to get drastically etched out (see Fig. 11c). The Raman spectra (Fig. 12), however, again show similarity to those of earlier RF–HF-CVD films where the substrate holder was the ground electrode. In this inverted electrode geometry, the ion-bombardment is expected to be intense due to the self-biasing effect in RF plasma and suppresses the crystal growth by producing disorder in the lattice of the nuclei seeds.

In conclusion, the coupling of RF plasma with the hot filament assisted CVD is observed to allow growth of

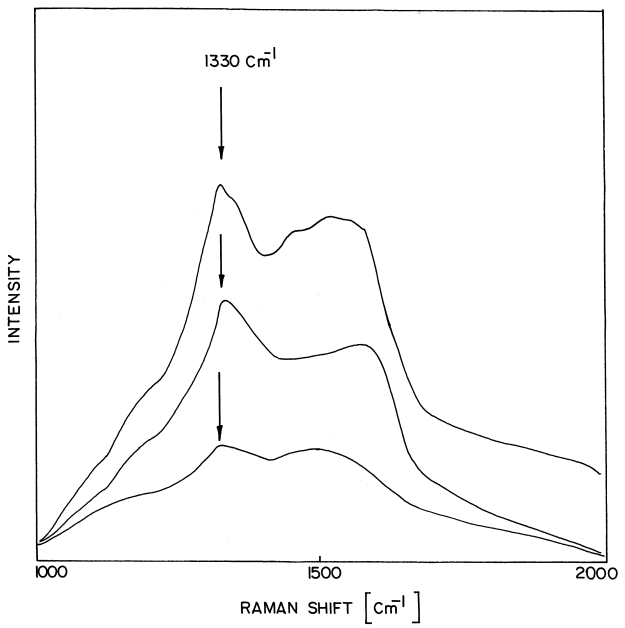

Fig. 12. Raman spectra of the diamond films deposited with the RF potential applied to the substrate holder: RF power: (a) 10 W, (b) 20 W and (c) 30 W.

diamond films at high pressure and low level of RF power with enhancement in the growth rate. The moderate RF power and low pressure lead to production of submicron microcrystalline particles imbedded in amorphous material. At higher levels of RF power at all pressures diamond films with needle-like morphology are formed. Addition of Ar to the source gas mixture at low levels of RF power produce change in orientation of crystallites from ⟨111⟩ to ⟨100⟩ planes. Thus our results suggest that more experimental work may be necessary to provide improved technique for the production of diamond films.

Acknowledgements

This work was partly supported by the Department of Science and Technology, Government of India, New Delhi under the DST Sanction No. III.5(18)/93-ET. NCL Communication No. 6422.

References

[1] A.T. Collins, E.C. Lightowler, The Properties of Diamond, in: J.E. Field (Ed.), Academic Press, San Diego (1979).
[2] M.W. Geis, Proc. IEEE 79 (1991) 669.
[3a] K.E. Spear, J. Am, Cer. Soc. 72 (1989) 171.
[3b] W. Zhu, R.B. Stoner, B.E. Williams, J.T. Glass, Proc. IEEE 79 (1991) 621.
[4] P.K. Bachmann, R. Messier, Chem. Eng. News 67 (1989) 24.
[5] D.S. Hoover, Scale-up and Commercial Applications of CVD Diamond and Diamond-like Materials, GAMI Conference on Diamond and DLC coatings, Marco Island, Florida (Oct. 15–17, 1989).
[6a] S.R. Lee, B. Gallois, Diam. Relat. Meter. 1 (1992) 235.
[6b] J.C. Angus, F.A. Buck, M. Sunkava, T.F. Groth, C.C. Hayman, R. Gat, MRS Bull. 14 (10) (1989) 38.
[6c] C. Angus, C.C. Hayman, Science 241 (1988) 913.
[7] P. Wood, T. Wydeven, O. Tsuji, in Program and Abstract of the First International Conference on the New Diamond Science and Technology, p. 100, New Diamond Forum, Tokyo, Japan (1988).
[8] S. Yugo, T. Kanai, T. Kimura, T. Muto, Appl. Phys. Lett. 58 (1991) 1036.
[9] J. Cui, R. Fang, Appl. Phys. Lett. 69 (1996) 3507.
[10a] A. Sawabe, T. Inuzuko, Appl. Phys. Lett. 46 (1985) 146.
[10b] A. Sawabe, T. Inuzuko, J. Cryst. Growth 137 (1986) 89.
[11] K. Kobashi, S. Karasawa, T. Watanabe, J. Cryst. Growth 99 (1990) 1211.
[12] H. Saitoh, T. Hirose, H. Matsui, Y. Hirotsu, Y. Ichinose, Surf. Coat. Technol. 39/40 (1989) 265.
[13] Z. Song, F. Zhang, Y. Guo, G. Chen, Appl. Phys. Lett. 65 (1994) 2669.
[14] A.A. Kumbhar, S.T. Kshirsagar, Thin Solid Films 283 (1996) 49.
[15] D.M. Bhusari, A.S. Kumbhar, S.T. Kshirsagar, Phys. Rev. B 46 (1993) 6460.
[16] D.M. Bhusari, A.S. Kumbhar, S.T. Kshirsagar, J. Mater. Res. 10 (1995) 1362.
[17] S. Matsumoto, Y. Sato, M. Tsutsumi, N. Setaka, J. Mater. Sci. 17 (1982) 3106.
[18] R. Messier, J. Vac. Sci. Technol. A 4 (1986) 490.
[19] K. Kobashi, K. Nishimura, Y. Kawate, T. Horiuchi, J. Vac. Sci. Technol. A 6 (1988) 1816.
[20] K. Kobashi, K. Nishimura, Y. Kawate, T. Horiuchi, Phys. Rev. B 38 (1988) 4067.
[21] S.A. Solin, A.K. Ramdas, Phys. Rev. B 1 (1970) 1687.
[22] R.J. Nemanich, S.A. Solin, Phys. Rev. B 20 (1979) 392.
[23] F. Tuinstra, J.L. Koenig, J. Chem. Phys. 53 (1970) 1126.
[24] R. Al-Jishi, G. Dresselhaus, Phys. Rev. B 26 (1982) 4514.
[25] P. Lespade, A. Mrchand, M. Couzi, F. Cruege, Carbon 22 (1984) 375.
[26] M. Yoshikawa, G. Katagiri, H. Ishida, A. Ishitani, Solid State Commun. 66 (1988) 1177.
[27] M. Ramsteiner, J. Wagner, Ch. Wild, P. Kordl, J. Appl. Phys. 62 (1987) 729.
[28] E.H. Lee, D.M. Hembree Jr., G.R. Rao, L.K. Mansur, Phys. Rev. B 48 (1993) 15540.
[29] N.H. Cho, K.M. Krishnan, D.K. Veirs, M.D. Rubin, C.B. Hopper, B. Bhushan, D.B. Bogy, J. Mater. Res. 5 (1990) 2543.
[30] N. Wada, S.A. Solin, Physica 105 (B+C) (1981) 353.
[31] R.E. Shroder, R.J. Nemanich, J.T. Glass, Phys. Rev. 41 (1990) 3738.
[32] J. Schwan, S. Ulrich, H. Roth, H. Ehrhardt, S.R.P. Silva, J. Robertson, R. Samlenski, R. Brenn, J. Appl. Phys. 79 (1996) 1416.
[33] S.J. Harris, A.M. Weiner, S. Prawer, K. Nugent, J. Appl. Phys. 80 (1996) 2187.